Supplementary information

The influence of hydroxide to fluoride substitution in trans-position to NO on the photochemistry of ruthenium nitrosyl complexes in solid state and solutions

Mikhailov A.A.[1], Brovko A.O.[2], Kuratieva N.V.[3], Eltsov I.V.[2], Schaniel D.[1], Kostin G.A.[3*]

[1]Universite´ de Lorraine, CNRS, CRM2, UMR 7036, Nancy 54000, France

[2]Novosibirsk state university, Pirogova 2, Novosibirsk, Russia, 630090

[3]Nikolaev institute of inorganic chemistry SB RAS, Lavrentieva 3, Novosibirsk, Russia, 630090

*Corresponding author, kostin@niic.nsc.ru
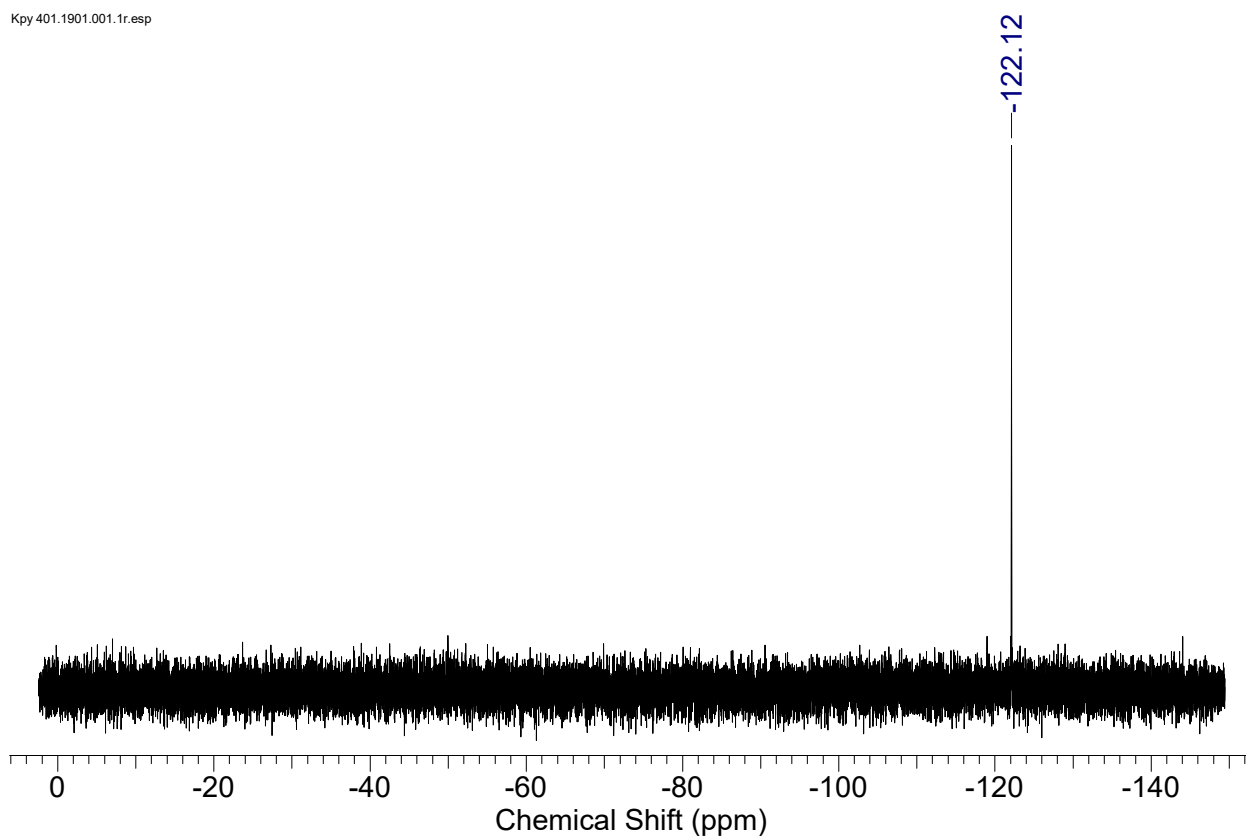
1. The identification of complex **1**.

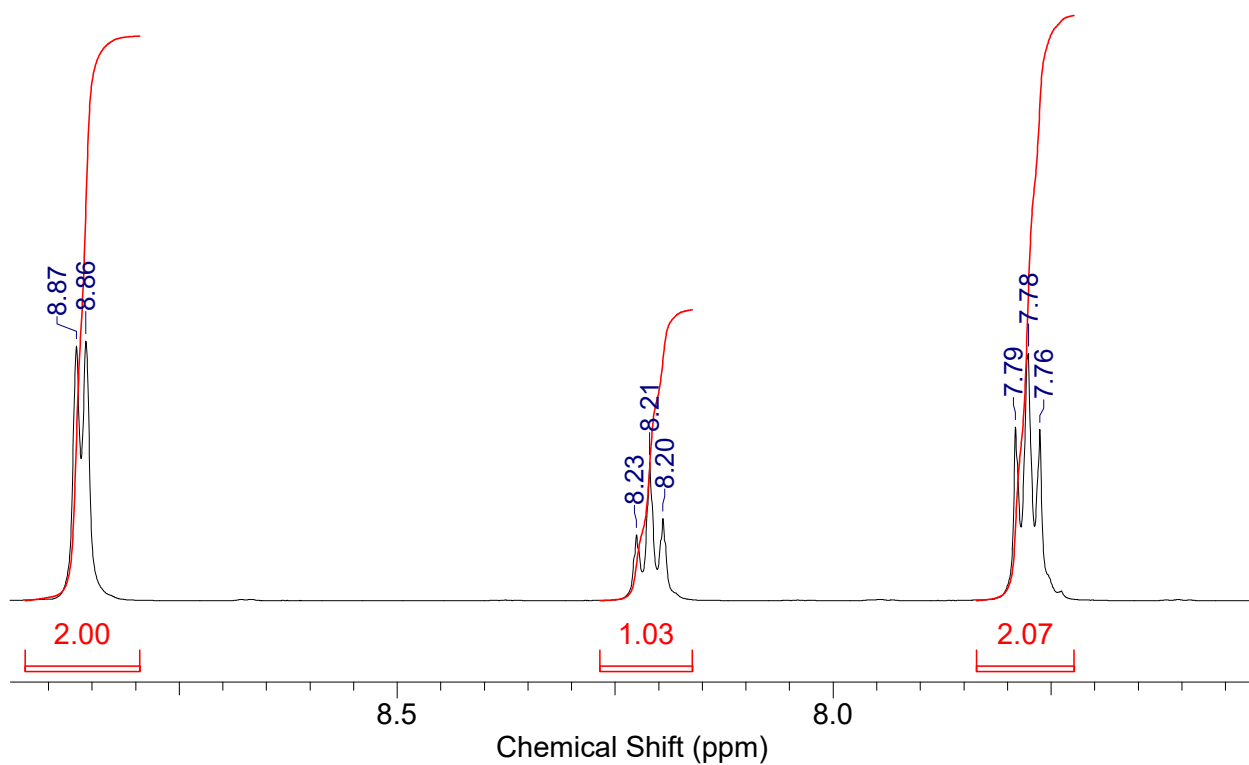Fig.S1.1. ^{19}F – NMR spectra of $[RuNOPy_2Cl_2F]$ (**1**).

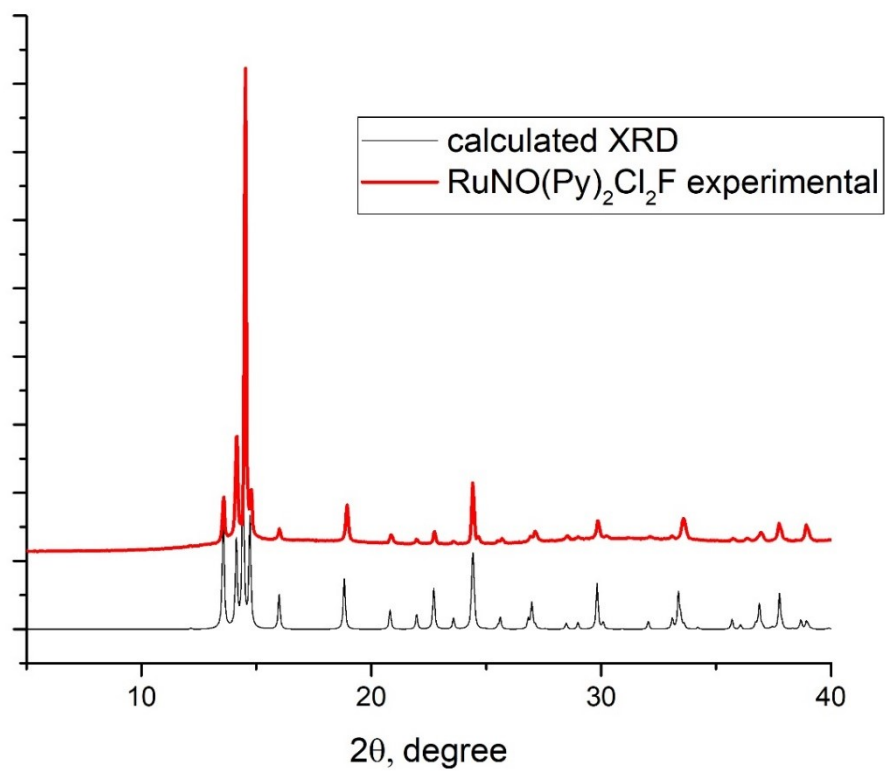Fig. S1.2. ^{1}H – NMR spectra of **1**.

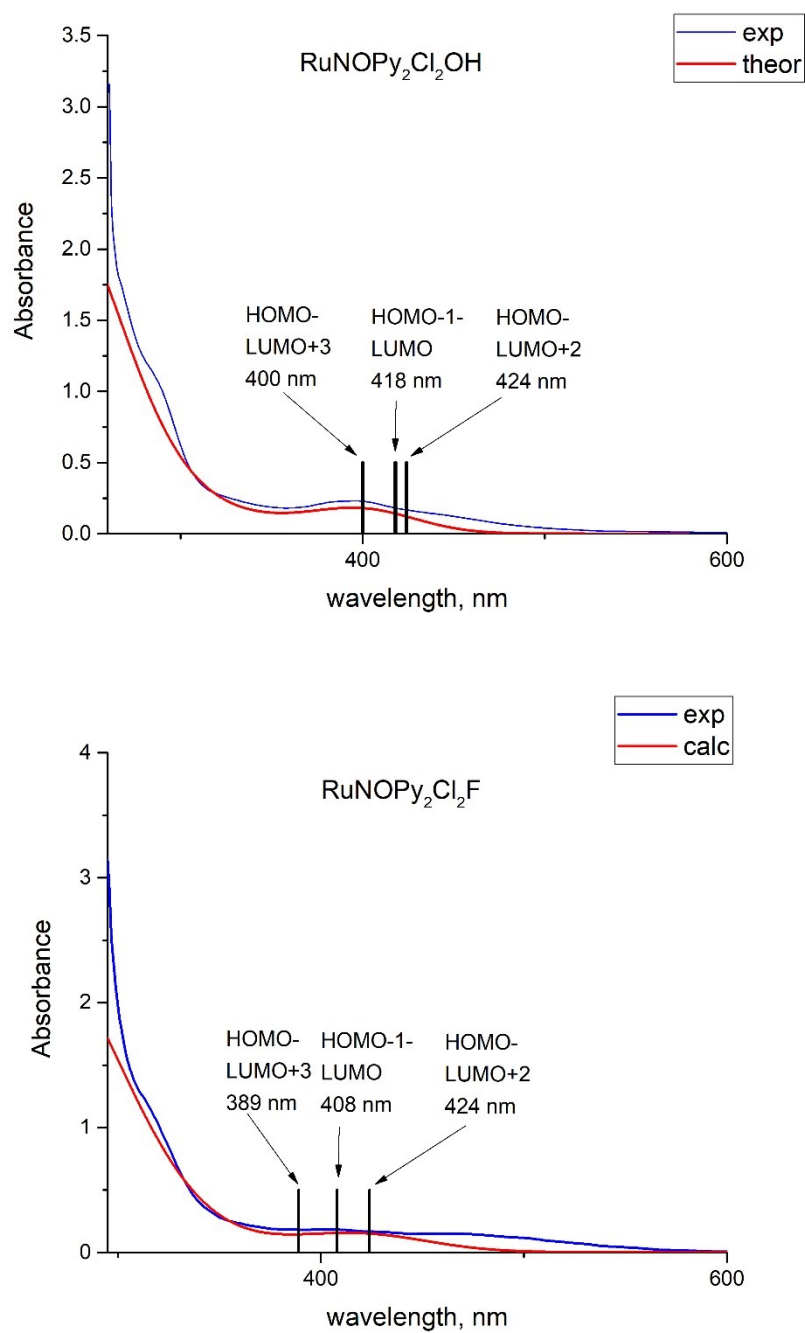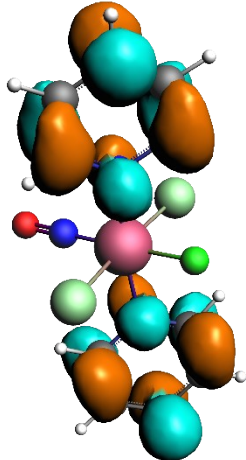Fig. S1.3. Calculated and experimental powder XRD data for **1**.

2. DFT calculations.
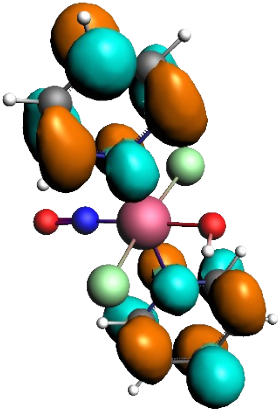
Fig. S2.1. Experimental and calculated spectra of investigated complexes. The calculated transitions in the rage of 400-450 nm are shown in bars.

Table S2.1. The frontier orbitals involved in the transitions at 400-450 nm in investigated complexes.

	[RuNOPy$_2$Cl$_2$F] (1)	[RuNOPy$_2$Cl$_2$OH] (2)
LUMO+3		
LUMO+2		
LUMO		

HOMO		
HOMO-1		

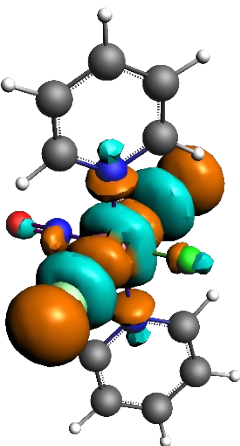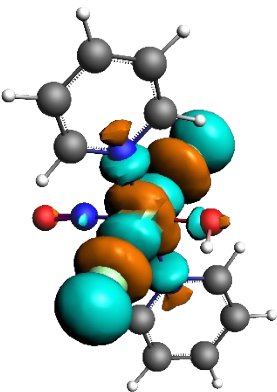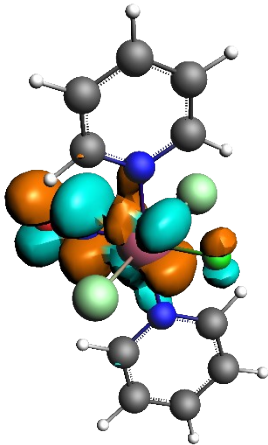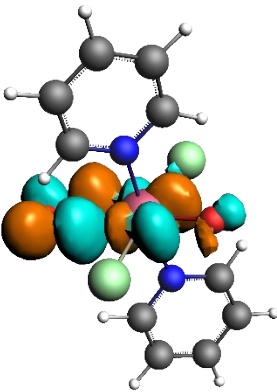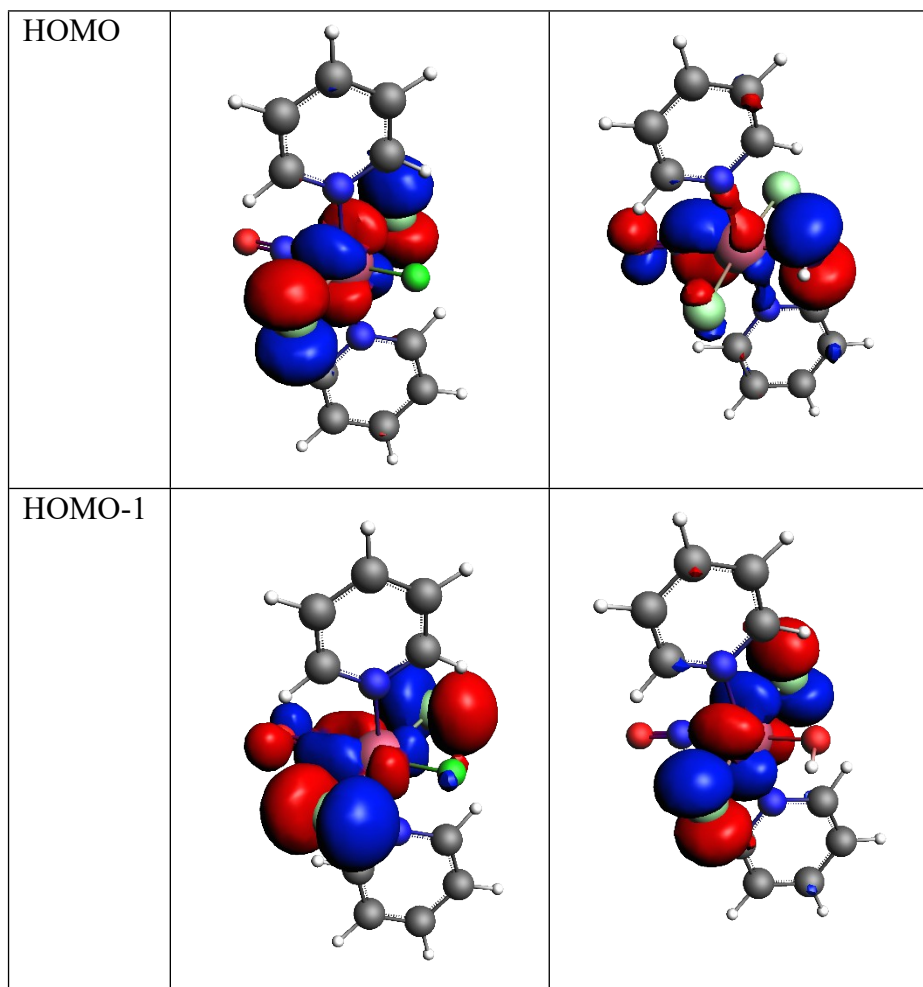Table S2.2.

Observed and calculated (in brackets) IR bands for [RuNOPy$_2$Cl$_2$OH] (**2**). The calculated bands were assigned according to the strongest oscillators.

Complex	Vibration	GS	MS1	MS2
2	ν(OH)	3537 (3636)	3504 (3622)	3496 (3572)
	ν(NO)	1824 (1821)	1674 (1748)	1522 (1509)
	δ(OH)	916 (888)	949, 939 (922)	991 (973)
	ν(Ru-OH)	575 (571)	624 (612)	- (594)
	δ(Ru-NO)	618 (624)	530 (527)	-
	ν(Ru-NO)	608 (603)	498 (489)	- (688)
	ρ(OH)	423 (425)	- (407)	491 (505)

3. Hirshfeld surface analysis.

Fig. S3.1. The Hirshfeld surface for [RuNOPy$_2$Cl$_2$F] (upper left) and two-dimensional fingerprints for the all (upper right), hydrogen (bottom left) and chlorine (bottom right) intermolecular interactions.

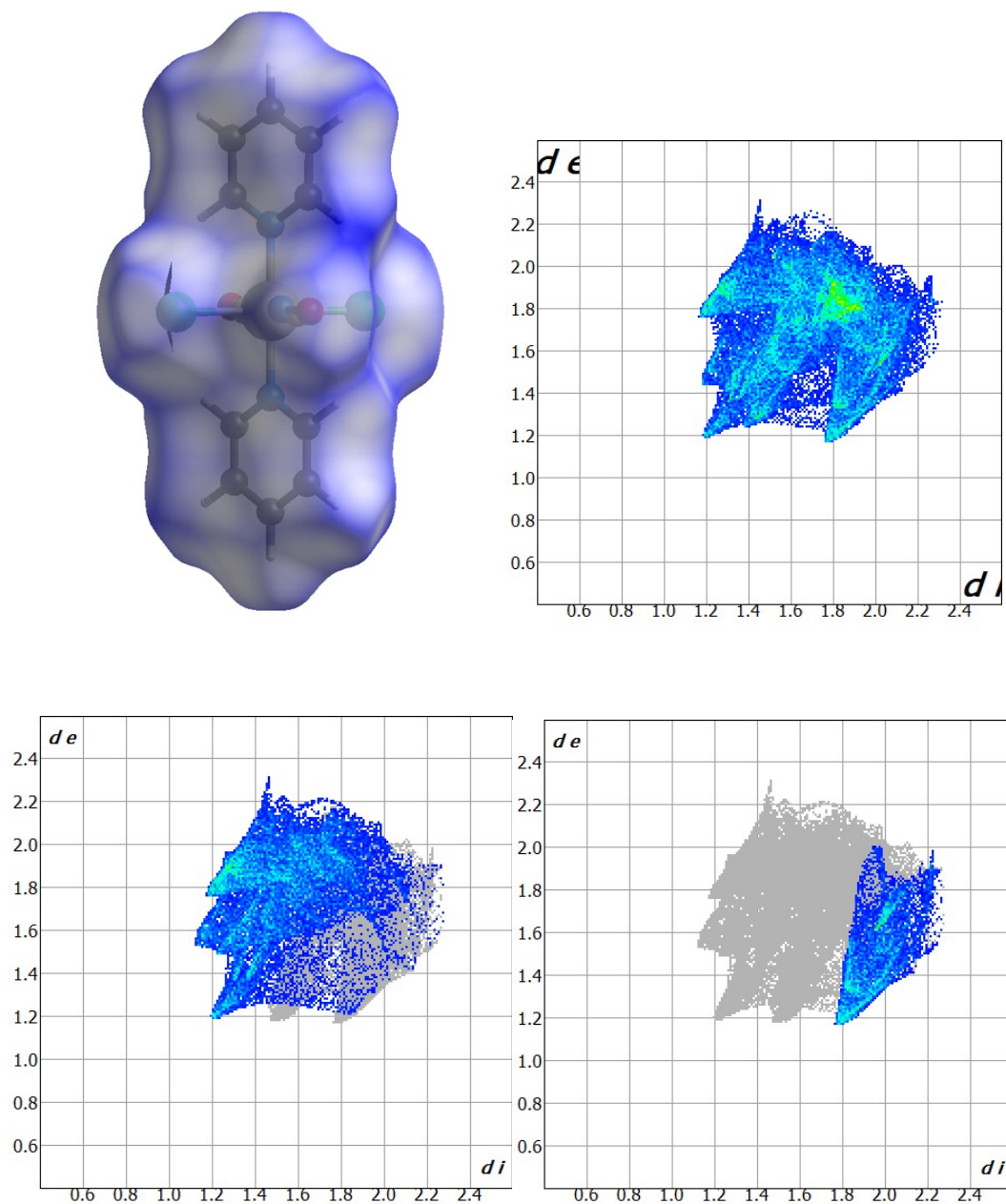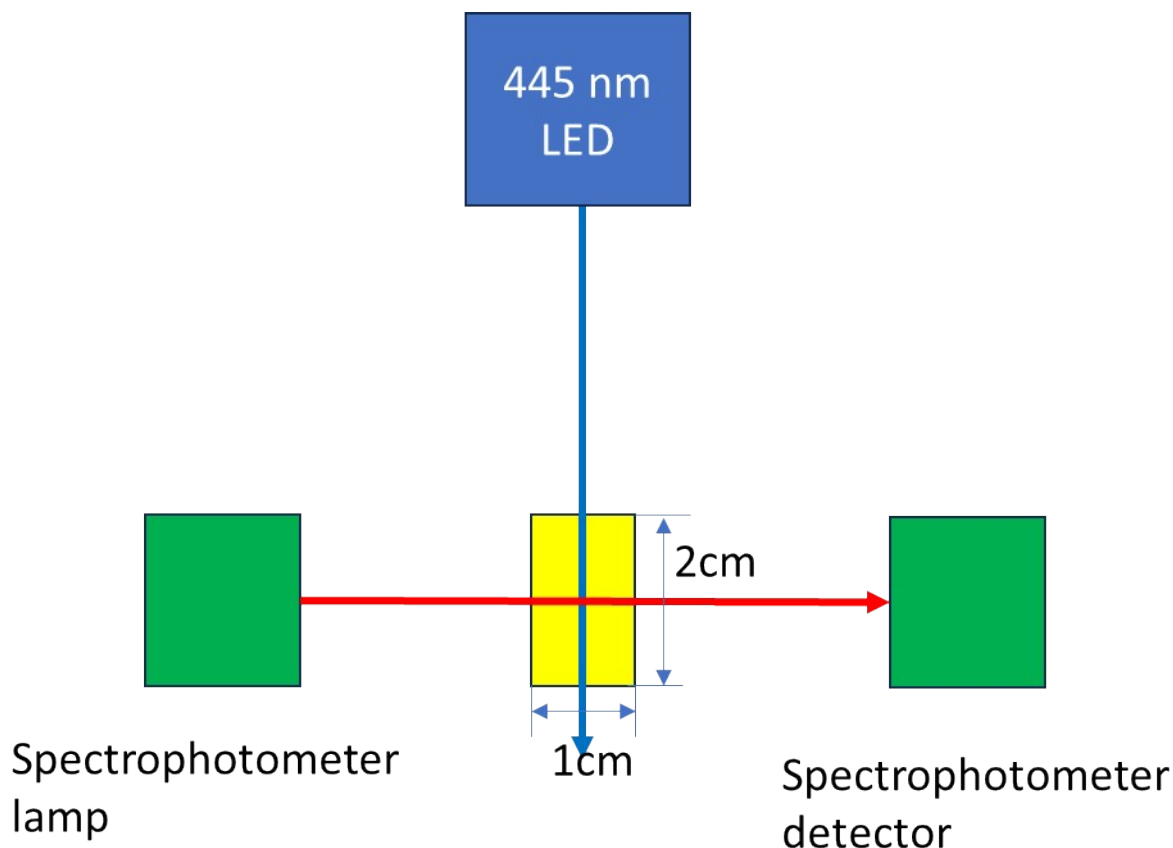4. Quantum yield calculations were performed according to E. Stadler, A. Eibel, D. Fast, H. Freißmuth, C. Holly, M. Wiech, N. Moszner, G. Gescheidt, *Photochem. Photobiol. Sci.* **2018**, *17*, 660–669. The LED irradiation was oriented perpendicular to the detection light pathway. See scheme S 4.1.

Scheme 4.1. The principal scheme of the experimental device. The pathway for the inducing irradiation is equal to 2 cm. The pathway for the detection light is equal to 1 cm.

4.1. Theoretical background.

The LED irradiation radiant power was recalculated to the photon flux I_0 (einstein·s^{-1}·L^{-1}) as follows:

$$I_0 = \frac{\lambda_{ex}P_{LED}}{hcN_aV} \quad (1)$$

where P_{LED} is the optical power of LED (W), λ_{ex} - the wavelength of LED irradiation (445 nm in our case), h – the Plank constant (J·c), c – the speed velocity (m/c), N_a – Avogadro number (mol^{-1}), V – volume of the solution under experiment ($2\cdot10^{-3}$ L in our case).

The time dependence of Reagent concentration is described by next formula:

$$\frac{d[R]}{dt} = -I_{absR}\Phi \quad (2)$$

where d[R]/dt – the change of the Reagent concentration (in mol/L), I_{absR} – the irradiation absorbed by the Reagent (einstein/(s·L)). Φ - the quantum yield.

In case of the transformation of one reagent to one product the molar absorption coefficients of Reagent (ε_R) and the Photoproduct (ε_P) and the optical path length l relate [R] to the observed changes of the absorbance (A) at a certain wavelength of spectra (370 nm in our case):

$$\frac{dA}{dt} = -I_{absR}\Phi(\varepsilon_R - \varepsilon_P)l \tag{3}$$

The absorbance at the zero time

$$A_0 = (\varepsilon_R)lC_0$$

and the absorbance after the complete conversion

$$A_\infty = (\varepsilon_P)lC_0$$

where C_0 – the initial concentration of Reagent.

Thus, the equation (3) can be transformed as

$$\frac{dA}{dt}C_0 = -I_{absR}\Phi(A_0 - A_\infty)/ \tag{4}$$

$$\frac{dA}{dt} = -I_{absR}\Phi(A_0 - A_\infty)/C_0$$

The link I_{absR} and I_0 can be established from Beer-Lambert equation

$$I_{abs} = I_0(1 - 10^{-Aex}) \tag{5}$$

where A_{ex} is the absorbance of the solution at the wavelength of excitation (455 nm). Generally the light can be absorbed by both the reagent and the product. Still in the initial point (see Eq. (6)) the light is absorbed only by the reagent and $I_{abs} = I_{absR}$. The value of A_{ex} can be determined from the initial spectra directly or as in our case can be calculated from previously established absorption coefficient of Reagent as:

$$A_{ex}(t = 0) = \varepsilon_R^{ex}C_0^R l_{ex}$$

where ε_R^{ex} – the absorption coefficient of Reagent at the LED wavelength, C_0^R – the initial concentration of Reagent, l_{ex} – the pathway for LED irradiation (2 cm).

For the low-absorbing solutions ($A_{ex} < 0.1$) the dependence of A(t) can be virtually fitted by mono-exponential kinetic $A = y_0 + A\cdot\exp(-kt)$, where y_0 corresponds to the A_∞, while A corresponds to the difference $A_0 - A_\infty$. In that case the derivative of the mono exponential fitting at $t = 0$:

$$\left(\frac{dA}{dt}\right)_{t=0} = -k_{fit}(A_0 - A_\infty) \tag{6}.$$

Combining (4) - (6) results in the equation for the quantum yield Φ:

$$\Phi = \frac{k_{fit} C_0}{I_{absR}} = \frac{k_{fit} C_0}{I_0 (1 - 10^{-Aex})}$$

4.2. Experimental results.

The typical A – t curves together with the exponential approximation are shown on Fig. S. 4.1 – S. 4.2.
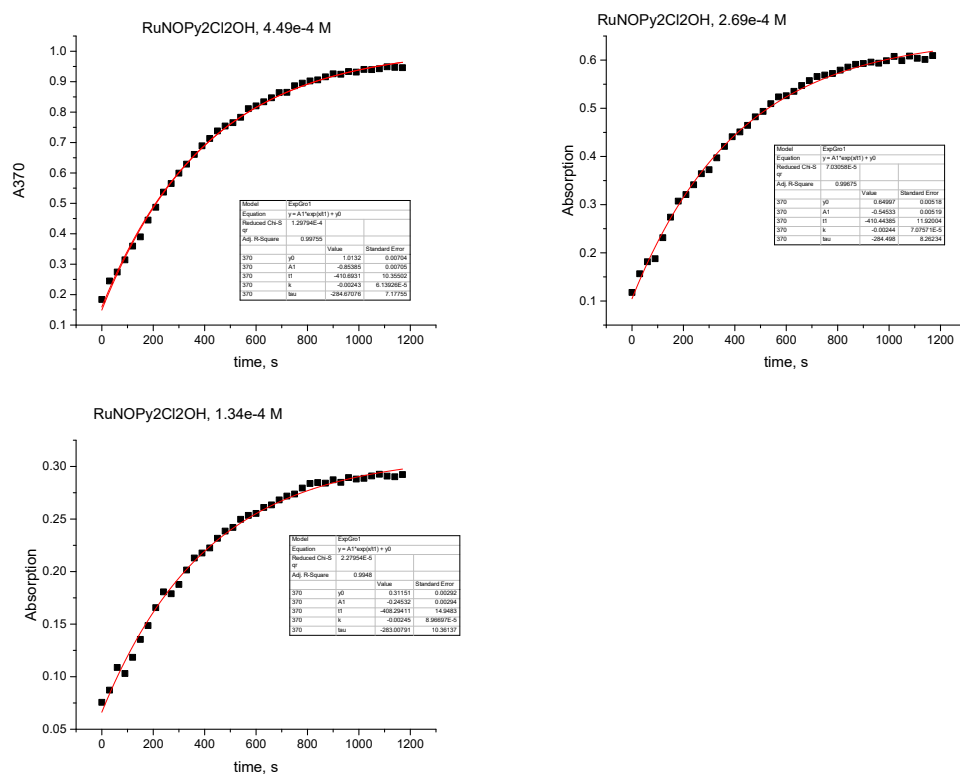

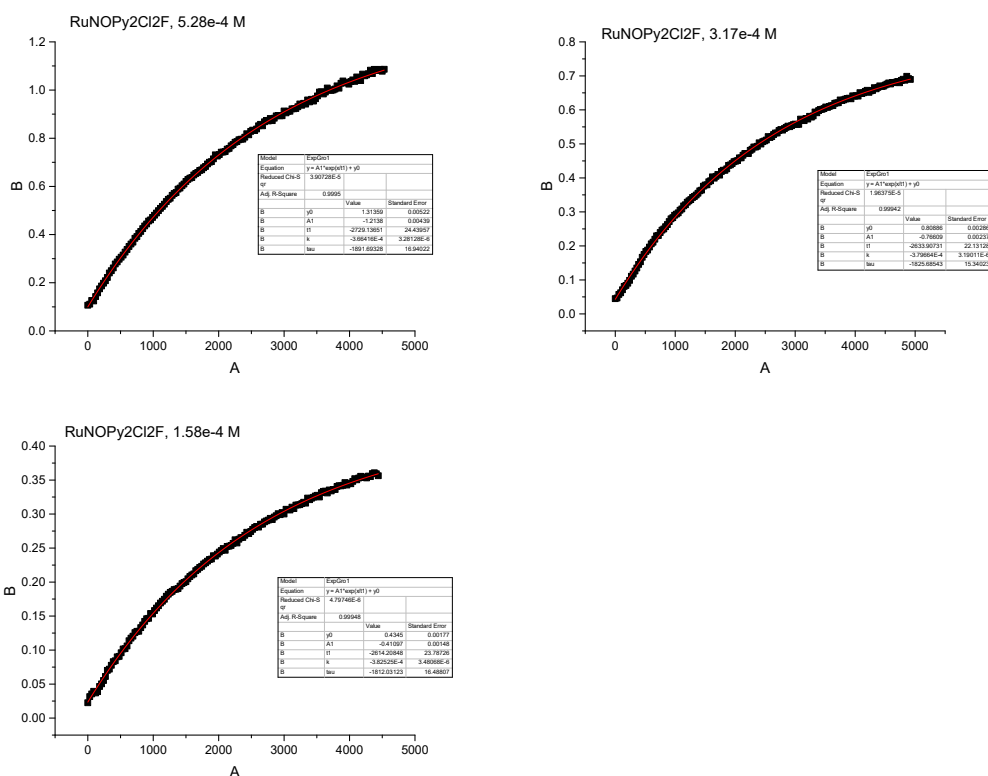Fig. S.4.1. The time dependencies of A_{370} for the different consentrations of [RuNOPy$_2$Cl$_2$OH].

Fig. S.4.2. The time dependencies of A_{370} for the different consentrations of [RuNOPy$_2$Cl$_2$F].

Table S4.1. The QY and corresponding fitting models for the complexes 1 and 2. I_0 was $1.88 \cdot 10^{-4}$ einstein·s^{-1}·L^{-1}. V = 0.002 L. l_{ex} = 2 cm, l_{reg} = 1 cm.

C_0, mol/L	k_{fit}, s^{-1}	$A_{ex(445\ nm)}$	λ_{reg}, nm	Fit equation	QY, %	QY, %
[RuNOPy$_2$Cl$_2$F] (**1**)						
$1.58 \cdot 10^{-4}$	$3.83 \cdot 10^{-4}$	0.024	370	A = 0.435-0.411exp(-0.000383t)	0.61	
$3.17 \cdot 10^{-4}$	$3.80 \cdot 10^{-4}$	0.048	370	A = 0.809-0.766exp(-0.000380t)	0.60	0.60±0.08
$5.26 \cdot 10^{-4}$	$3.36 \cdot 10^{-4}$	0.080	370	A = 1.314-1.213exp(-0.000336t)	0.61	
[RuNOPy$_2$Cl$_2$OH] (**2**)						
$1.34 \cdot 10^{-4}$	$2.45 \cdot 10^{-3}$	0.029	370	A = 0.311-0.245exp(-0.00245t)	2.70	
$2.69 \cdot 10^{-4}$	$2.44 \cdot 10^{-3}$	0.059	370	A = 0.650-0.545exp(-0.00244t)	2.76	2.78±0.16
$4.49 \cdot 10^{-4}$	$2.43 \cdot 10^{-3}$	0.099	370	A = 1.013-0.853exp(-0.00243t)	2.89	

The QYs calculated according to model described are independent on concentration as it should be. The parameters of fitting (y_0, A) linearly depends on the concentration that also indirectly proof the correct model.

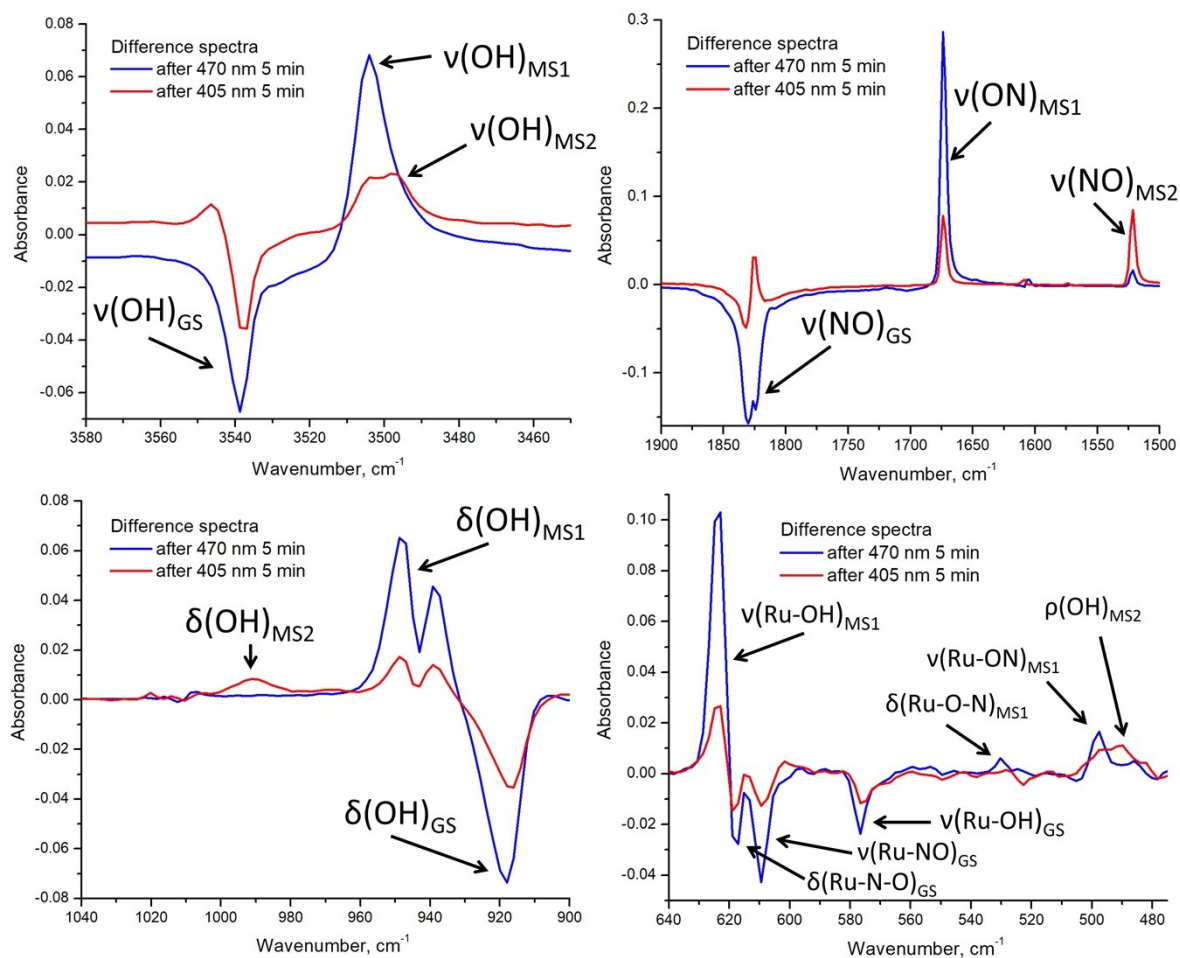## 5. IR spectroscopy for the solid state isomerization.

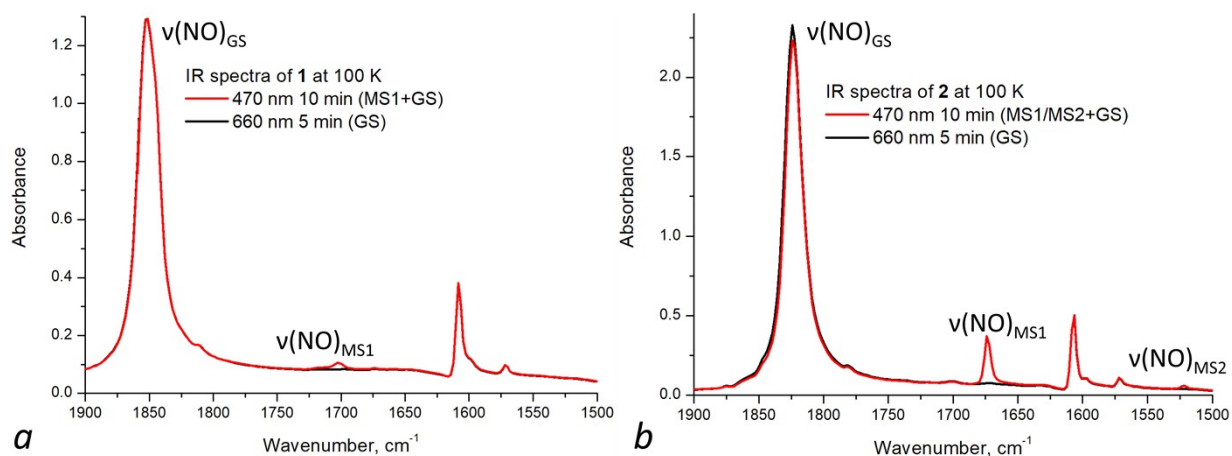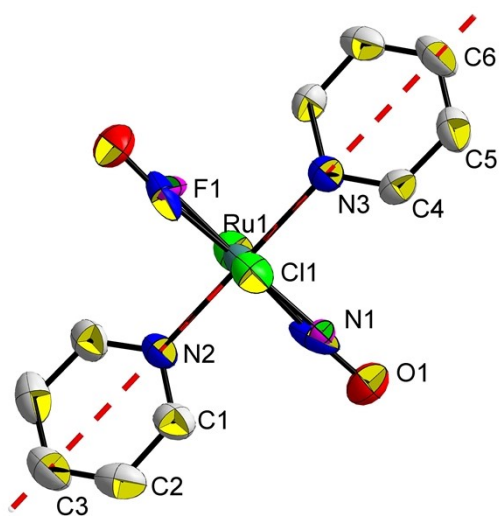Fig. S5.1. Difference IR-spectra of **2** before (GS) and after irradiation (at 470 or 405 nm) at 100 K.

Fig. S5.2. Solid-state IR-spectra of **1** (panel *a*) and **2** (panel *b*) measured at 100 K after light irradiation at 470 and 660 nm.

6. The crystal structure of [RuNOPy$_2$Cl$_2$F]

a

Fig. S. 6.1. The molecular fragment of [RuNOPy$_2$Cl$_2$F]. The NO group and F-ligand are disordered in two positions with 50 % population.